Dependence of ZrN coating failure of U-Mo particle on coating thickness at high temperature

Ji-Hyeon Kim[a], Sunghwan Kim[b], Kyu Hong Lee[b], Lee Chong-Tak[b], Dong-Seong Sohn[a]*
[a] *Ulsan National Institute of Science and Technology, 50 UNIST-gil, Eonyang-eup Ulju-gun, Ulsan, 689-798, Korea*
[b] *Korea Atomic Energy Research Institute, 111, Daedeok-daero 989beon-gil, Yuseong-gu, daejeon, Republic of Korea*
[*] *Corresponding author: dssohn@unist.ac.kr*

1. Introduction

U–7wt.% Mo dispersion fuel with high fuel density of ~55vol.% was proposed to apply into high performance research reactor. However, it has been detected undesired interaction phase between U-Mo fuel and Al matrix depressing fuel safety in high burnup operating in research reactor. In order to suppress the undesired interaction layer, diffusion barrier coating has been suggested. Zirconium nitride (ZrN) is one of promising diffusion barrier materials which has good properties. IV-B transition metal nitride like ZrN, TiN and HfN belongs to NaCl or A15 structure which has high melting temperature and extream stability in hardness and chemical inertness [1]. IV-B transition metal nitride is applied in broad fields as protective coating due to their useful properties such as corrosion, hardness, abrasion resistance, wear resistance, abrasion resistance, decorative potential and chemical stability [2]. Also ZrN coating has shown good performance as diffusion barrier in U-Mo dispersion fuel. However in annealing test [3,4], heavy ion test [5] and in-pile test [6], some local damages in the ZrN coating of as-fabricated plate fuel worked as fast diffusion path for Al and induced the significant interaction phase with fuel. It is assumed that these cracks are formed from fuel-plate-fabrication process [5,6].

It is important that ZrN coating maintains the integrity under fuel-plate-fabrication process to work as diffusion barrier properly. Stresses sources arousing coating failure have been expected as external mechanical loads during rolling step or dimensional change resulting from different coefficient of thermal expansion (CTE) between substrate and coating at specific temperature [4,6]. Especially brittle ceramic materials are difficult to maintain coating integrity due to relatively large change in properties of the metallic substrate and the ceramic coating at high temperature [7]. Irradiated SELENIMM plates were produced at below 450℃, but fuel plate with hard Al-6061 (AA6061) cladding generally fabricated at as high as 500℃ [5]. Heating of fuel-plate-fabrication process carries out at pre-heating before hot rolling process and blister test and heating time is almost 2h in total.

There have been few studies that have attempted to prove the effect of each stress origins. So this paper seeks to evaluate the effect of thermal stress resulting from different thermal expansion coefficient between substrate and coating under isothermal condition on integrity of ZrN coating on U-7Mo powder. Also this study identifies and addresses coating failure problem with coating thickness and annealing temperature. Surface and cross sectional morphology of unannealed and annealed samples were characterized with Scanning Electron Microscope (SEM) coupled with Energy Dispersive X ray Spectrometer (EDS). Structure information was analyzed by X-Ray diffractometer (XRD).

2. Methods and Results

U–7Mo powders were produced via centrifugal atomization in the Korean Atomic Energy Research Institute (KAERI) [8] and stored in the air. ZrN coating was deposited on the U–7Mo powders in the range of 45 to 90μm by DC sputtering deposition system. Powders were rotated continuously in turning drum for uniform thickness during deposition. Deposition condition was: (1) rectangular ZrN target with purity of 99.5%; (2) base pressure of $3*10^{-5}$torr; (3) working pressure of $1.5*10^{-3}$ torr; (4) deposition substrate temperature of about 250℃; (5) power of 1 kW; (6) mixing drum speed of about 4 rotations per minute; and (7) distance of 17 cm between target and substrate. Deposition temperature was measured at surface of DU-7Mo ingot sample by K type thermocouple under the deposition condition without rotation. After several minutes of deposition, temperature met saturation at 250℃. ZrN of 0.2, 0.5, 0.8, 1.1, 1.7, 2.2, 2.6μm was coated on U-Mo powders by controlling the deposition time from 2 to 25h. All ZrN coated powders were annealed at 500℃ for 2h. Annealing test was conducted under vacuum atmosphere of $3*10^{-5}$ mbar. Slow heating rate of 16.7 ℃/min and power off cooling were employed to avoid coating cracking from rapid temperature change. For cross section analysis of sample, mounted samples were polished upto 1μm and followed by ultrasonic cleaning with ethanol and then characterized with Scanning Electron Micrography (TESCAN VEGA3) coupled with Energy Dispersive X ray Spectrometer (Oxford INCA x-act). Microscopic analysis used backscattered electron (BSE) images of surface and cross sectional sides. For compositional and structural analysis, X-Ray diffractometer (RIGAKU ULTIMA IV) with Cu-K(α) radiation (λ = 1.5406 Å, a accelerating voltage of 40 kV, a current of 30 mA). X-Ray Diffraction patterns covered the range of 2θ = 20-140° with a θ/2θ mode, 0.02 step and a step time of 10s.

A divergence slit of 10 mm and receiving slit of 0.6 mm were used. XRD calibration was conducted by using (111) reflection plane (2θ = 28.44° with CuKα1 radiation) of silicon standard material. As a guide of NIST SRM 640, XRD instrument was adjusted to satisfy a full width at half maximum (FWHM) for 0.10° of 2θ or less and position shift within 2θ = 0.01°. All the XRD patterns were analyzed with PDXL 2 program using the Rietveld method.

3. Result & Discussion

3.1 Origin of coating failure

At high temperature of post-deposition annealing processes in this study, thermal stress is likely to dominate over intrinsic stress [9]. When a coated substrate is at a temperature that is different from its deposition temperature, a thermal stress will result from the discrepancy in CTE between the film and substrate. For homogeneous materials without temperature gradients and bending, a simple equation under a one-dimensional approximation to estimate the thermal stress can be represented as below equation. The equation is able to be simplified if the coating thickness (t_c) is much smaller than the substrate thickness (t_s).

$$\sigma_{th} = \frac{E_c(\alpha_s - \alpha_c)(T_S - T_a)}{(1 - v_c)(1 + \frac{2t_c E_c}{t_s E_s})} \approx \frac{E_c(\alpha_s - \alpha_c)(T_S - T_a)}{1 - v_c}$$

where E_c and E_s are Young's modulus of coating and substrate in P_a, α_c and α_s are the CTE for the coating and substrate in K^{-1}, T_s is the substrate surface temperature during deposition, and T_a is the temperature during measurement. A positive value of σ_{th} corresponds to tensile stress, while a negative means compressive stress. As shown in Table 2, calculated thermal stress is same as total stress due to zero intrinsic stress calculated by Halder–Wagner equation. The calculation applied measured deposition temperature of 250℃, Young's modulus of 450MPa [10], CTEs of 7.24 * 10^{-6} K^{-1}[11] and 15.6 * 10^{-6} K^{-1} [12] for coating and substrate. For annealing above deposition temperature of 250℃, tensile stress creates over coating and develops proportionally to annealing temperature. Therefore, higher annealing temperature is highly likely to induce coating failure.

3.2 Effect of coating thickness on coating failure

Fig. 1 presents U-7Mo powder coated poly crystalline ZrN. Measured averages and standard deviations of each coating thickness are noted in table I according to deposition time. The coating thicknesses mostly have standard error of several decades nanometer. To obtain the accurate values, thickness was deduced by measuring coated powders which satisfied diameter range of 45-90μm in cross sectional SEM images. 0.2,

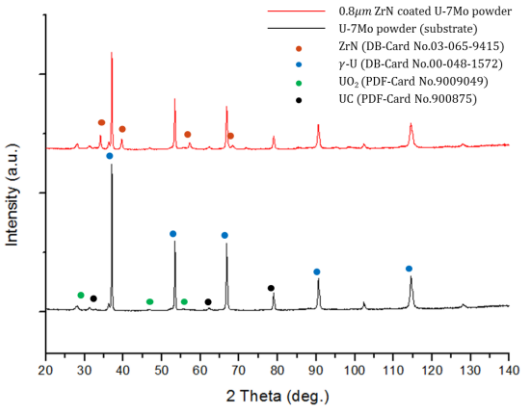

Fig. 1. XRD result of 0.8 um ZrN coated U-7Mo powder comparing with U-7Mo substrate powder

0.5, 0.8, 1.1, 1.7, 2.2, 2.6μm ZrN coated U-Mo powders were annealed at 500℃ for 2h. Fig. 2 is surficial and cross sectional BSE images of 2.6μm coated U-Mo particles after annealing at 500℃ for 2h. Annealed specimens displayed through-thickness cracking as shown in Fig. 2(a). Surface image of Fig. 2(b) shows that cracks propagated through column boundaries and form crack channeling with polygonal pattern. The polygonal pattern of cracks proves isotropic tensile stress for in-plane direction of coating [13-15]. Under high isotropic tensile film stress, microcracking is produced and the cracks tend to meet orthogonally and generate polygon islands or chips like dried mudflats. Cracks tended to initiate and propagate at weak points of coating like interfaces of columns, hillocks and pin-holes.

The coating thickness plays an important factor for coating failure as well as elastic modulus, morphology and the density of film. By analyzing the surficial and cross sectional images of annealed samples, it was certified that the coating integrity of 0.2μm coating maintained, while thick coating above 0.5μm had through-thickness cracks of polygonal pattern. 0.5μm coating displayed the mixed mode of cracked and non-cracked coating. So it can be suggested that critical value is about 0.5μm for safe-fail design of ZrN coating on U-Mo fuel. Since coating thickness tended to be thicker as substrate size increases, relatively thick coating on bigger substrate within particles coated with mean 0.5μm thickness might suffer the fracturing.

The dependence of coating fracturing on thickness results from stress distribution along thickness. Stress in coating under high temperature is induced dominantly by thermal stress from CTE mismatch between substrate and coating [16]. ZrN coating of 7.24 * $10^{-6}K^{-1}$[11] is greater than U-Mo substrate of 15.6 * $10^{-6}K^{-1}$[12].

Coating morphologies such as interfacial defect, border, curved surface and crack substantially affect the stress

Table II: Coating thickness and annealing results at 500℃ of fabricated ZrN coated U-Mo powders as a function of deposition time

Deposition time (h)	Average thickness (nm)	Standard deviation (nm)	Film failure after annealing at 500℃
2	189	20	No cracking
4	471	42	Mixed with non-cracked and through-thickness cracked particles
7	840	41	Through-thickness cracking
10	1082	37	
13	1694	54	
15	2246	70	
25	2582	224	

gradient within coatings [18-21]. Especially spherical substrate with curved surface results in a variation of the stress along the thickness direction of ZrN coating. So compressive stress are applied in substrate, while tensile stress in film. From inner to outer surface of coating induced positive strain rises due to spherical shape of samples and thus tensile stress naturally increases. It is assumed that bonding between coating and substrate maintains. Surface BSE images of samples annealed at 500℃ for 2h showed that coating above 0.5μm thickness were cracked. Maximum normal stress theory [17] states that a brittle material fails when the maximum principal stress exceeds some value, independent of whether other components of the stress tensor are present. Thus maximum principal stress near surface of 0.5μm coating is expected to be close to stress value for fracturing. Also stress induced cracks show different failure mode affects adhesion between the coating and the substrate. Coating with above 1.7μm showed mixed-mode failure which is a combination of both cohesive and adhesive failures, whereas coating below 1.7μm presented only adhesive fracturing. As a result of stress gradient, thick coating with the thickness beyond specific value is likely to produce cohesive failure as well as fracture. The stress translates between the coating and the substrate by shear at the interface, causing the coated systems to contract, elongate or bend [22].

4. Conclusion

Integrity of ZrN coating on U-Mo particle at 500℃ was evaluated as a function of coating thickness based on SEM analysis. Thermal stress as a result of the differences in CTE between coating and substrate plays

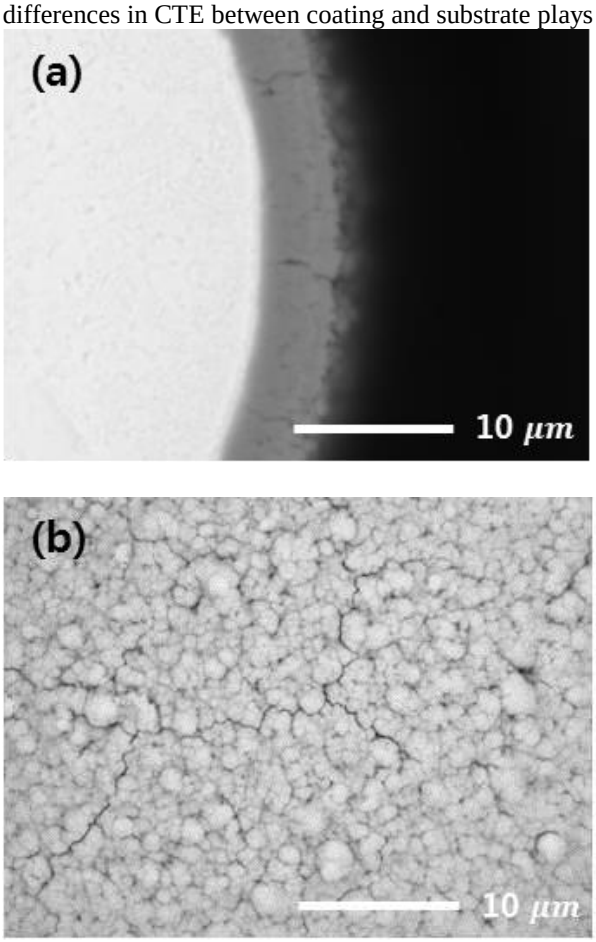

Fig. 2. Cross sectional (a) and surficial (b) BSE images of 2.6μm ZrN coated U-Mo powder

a role in the fracturing of coating layer. Under heat-treatment at 500℃ for 2h, tensile stress in ZrN coatings with above critical thickness of 0.5μm exceeded the true toughness of coating and induced fracturing. The annealed coating presented microcracking with a pattern of polygonal islands or chips as a result of high isotropic tensile in in-plane film stress. The cracks generated through interfaces of columns, hillocks and holes.

REFERENCES

[1] Ribarsky, M. W., and E. D. Palik, "Handbook of optical constant of solids." Titanium Dioxide (TiO2)(Rutile) (1985): 795-804

[2] PURANDARE, Yashodhan, EHIASARIAN, Arutiun, SANTANA, Antonio, HOVSEPIAN, Papken (2014). ZrN coatings deposited by high power impulse m
agnetron sputtering and cathodic arc techniques. Journal of Vacuμm Science & Technology A, 32 (3).

[3] T. Zweifel, H. Palancher, A. Leenaers, A. Bonnin, R. Tucoulou, S. Van Den Bergen, R. Jungwirth, F. Charollais, W. Petry, J. Nucl. Mater. 442 (2013) 124–132.
[4] S.V. den Berghe, A. Leenaers, C. Detavernier, The SELENIMM fuel experiment – progress report after two cycles, in: Proceedings of the International Meeting on Reduced Enrichment for Research and Test Reactors (RERTR), Warsaw, 2012.
[5] Jungwirth, T. Zweifel, H.Y. Chiang, W. Petry, S. Van den Berghe, A. Leenaers, Nucl. Mater. 434 (2013) 296–302
[6] A. Leenaers, S. Van den Berghe, E. Koonen, V. Kuzminov, C. Detavernier, J. Nucl. Mater. 458 (2015) 380–393.
[7] National Research Council. Coatings for high-temperature structural materials: trends and opportunities. National Academies Press, 1996.
[8] Ki Hwan Kim, Don Bac Lee, Chang Kyu Kim, Gerard E. Hofman, Kyng Wook Park, J. Nucl. Mater. 245 (1997) 179–184.
[9] A. Thornton, D. W. Hoffman, Thin solid films 171 (1989) 5-31.
[10] DB card No. 03-065-9415.
[11] Cheng-Shi Chen, Chuan-Pu Liu, C.-Y.A. Tsao, Heng-Chieh Yang, Scripta Mat. 51 (2004) 715–719.
[12] Thermophysical Properties of U-10Mo Alloy, INL/EXT-10-19373
[13] K. Ogawa, T. Ohkoshi, T. Takeuchi, T. Mizoguchi, T. Masμmoto, Jpn. J. Appl. Phys. 25 (1986) 195.
[14] R. Pestrong, "Nature's Angle," Pacific Discovery—California Academy of Sciences 44(3):28 (Summer, 1991) 20.
[15] Ghyka, M. Costiescu, The geometry of art and life, Courier Corporation, 1946.
[16] E. Cuthrell, F. P. Gerstile Jr, D. M. Mattox, Rev. Sci. Instrum. 60 (1989) 1018-1020.
[17] Rankine, W. J. Macquorn, Philosophical Transactions of the Foyal Society of London 147 (1857) 9-27.
[18] E. Suhir, J. Appl. Mech. 55 (1988) 143-148.
[19] J. T. Drake, R. L. Williamson, B. H. Rabin, J. Appl. Phys. 74 (1993) 1321-1336.
[20] A. G. Evans, W. Hutchinson, Acta Metall. Mater. 43 (1995) 2507–2530
[21] S. M. Hu, J. Appl. Phys. 50.7 (1979): 4661-4666.
[22] V. Teixeira, Vacuum 64 (2002) 393–399